Impacts of Crest Factor Reduction and Digital Predistortion on Linearity and Power Efficiency of Power Amplifiers

Siqi Wang, Morgan Roger, Caroline Lelandais-Perrault

Impacts of Crest Factor Reduction and Digital Predistortion on Linearity and Power Efficiency of Power Amplifiers

Siqi Wang, Morgan Roger, Caroline Lelandais-Perrault

***Abstract*—The linearity and power efficiency are two main factors of power amplifiers (PA), which can hardly be improved together. Digital predistortion (DPD) compensates for nonlinearity and memory effects of PAs in high efficiency zone. However, for advanced communication standards the high peak-to-average power ratio of the modulated signal constrains the PA operating point and thus limits the power efficiency. Crest factor reduction (CFR) techniques are applied to address this problem though they degrade the PA linearity relatively. In this paper, we compare different CFR approaches with respect to their performances in terms of linearity, PA power efficiency, and computational complexity. Classical hard clipping, clip-and-filter as well as joint CFR/DPD methods are considered. To complete the comparison, we propose a modeled CFR identified using indirect learning architecture combined with DPD. The simulation results validate its effectiveness on the trade-off among linearity, PA power efficiency and CFR computational complexity.**

***Index Terms*—Digital predistortion, crest factor reduction, nonlinear distortion, power amplifiers, power efficiency**

I. Introduction

POWER amplifiers (PA) are one of the most power consuming components in radio frequency (RF) telecommunication systems. However, operating points with high power efficiency are always near the saturation zone, where PAs are very nonlinear. Digital predistortion (DPD) is an efficient choice to linearize the PA [1]. It has the inverse characteristics of the PA and is applied upstream of the PA in a transmitter circuit [2].

With the linearization by DPD, the PA is allowed to operate near the edge of its saturation zone with high efficiency and good linearity. Yet the operating point is still constrained by the peak-to-average power ratio (PAPR) of the modulated signal [3]. In order to make sure that no part of the signal is saturated, we need to impose an output back-off (OBO) at least equal to the PAPR, which may decrease the PA power efficiency [4].

Crest factor reduction (CFR) techniques are cost-effective methods to reduce PAPR. The conventional approach is to directly clip the samples that exceed the threshold and is called hard clipping (HC). But this generates both in-band and out-of-band distortion on the signal [5]. To remove out-of-band components, the clip-and-filter approach (CAF) applies a filter on the correction signal which is the difference between the original signal and the clipped signal. It trades off in-band errors for reduced out-of-band errors.

Some other approaches without in-band (error vector magnitude) degradation have been proposed, e.g. partial transmit sequence (PTS) and selective mapping (SLM). But they need to transmit side information so that the receiver can recover the modulated signal, which reduces the throughput [6].

In the literature, the CFR is most often applied independently in front of DPD. Sometimes a joint approach for DPD and CFR is used, such as in [7] where a modeled CFR (MCFR) is proposed and is applied on the output signal of the DPD. The DPD coefficients and the MCFR coefficients are identified separately.

Though there have been several studies of CFR/DPD combinations as introduced above, they scarcely focus on the trade-off among linearity, PA power efficiency and CFR computational complexity. In this paper, we compare the impacts on linearity and PA power efficiency of different approaches by applying the CFR behind or in front of the DPD. The complexity of their implementations is also considered. The model in [7] is identified using closed-loop direct learning architecture (DLA). In order to complete the comparison of CFR approaches, we propose an approach to identify the MCFR using indirect learning architecture (ILA).

This paper is organized as follows. In Section II we present the algorithms used for DPD and CFR. An MCFR identified by ILA is proposed in Section III to complete the comparison of CFR approaches. Section IV estimates the complexity of each CFR approach. In section V, the simulation results are presented and discussed. Finally, the conclusion is given in section VI.

II. DPD and CFR

A. DPD and identification architectures

Different models derived from Volterra series have been used as DPD in the literature because the identification of their coefficients can be solved as a linear problem. If $\boldsymbol{\beta}$ denotes the vector of N_c coefficients, the vector of DPD output signal samples is

$$\boldsymbol{x} = \boldsymbol{\Phi_u}\boldsymbol{\beta} \tag{1}$$

where $\boldsymbol{\Phi_u}$ is the $N \times N_c$ matrix of basis functions for the DPD input signal $\boldsymbol{u} = [u(1), ..., u(N)]^T$, with N the number of signal samples. The DPD model can be identified using direct learning architecture or indirect learning architecture

The authors are with GeePs — Group of electrical engineering - Paris, UMR CNRS 8507, CentraleSupélec, Univ. Paris-Sud, Université Paris-Saclay, Sorbonne Université 3 & 11 rue Joliot-Curie, Plateau de Moulon 91192 Gif-sur-Yvette CEDEX, France (e-mail of authors: first-name.surname@centralesupelec.fr).

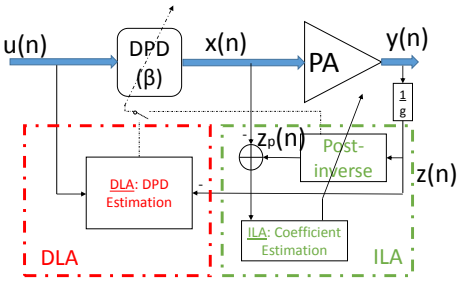

Fig. 1: DLA and ILA structures

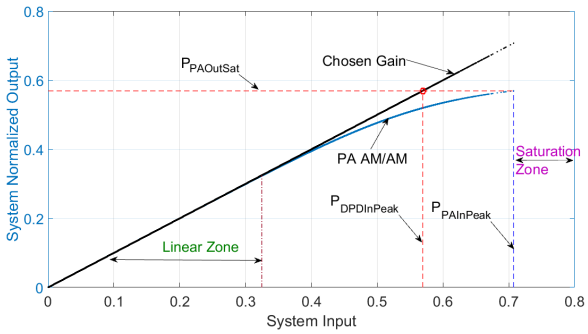

Fig. 2: PA output signal vs PA input signal

[8] as shown in Fig 1. Both learning architectures use the feedback signal $z(n)$, which is the PA output $y(n)$ normalized by the chosen gain g of the linearized PA. As different possible choices for g achieve about the same PA efficiency [9], we choose the small signal gain in this paper.

Before the DPD can be identified, the PA saturated output power P_{PAoutSat} needs to be characterized, as illustrated in Fig 2. The maximum DPD input peak power $P_{\mathrm{DPDinPeak}}$ can then be obtained by dividing P_{PAoutSat} by g. The maximum PA input peak power P_{PAinPeak} is defined by its corresponding output power being the edge of the PA saturation zone.

1) DLA: We present here the closed-loop DLA used in [7]. The DPD coefficients are estimated iteratively. At the i-th iteration, the bias $\Delta\boldsymbol{\beta}$ of DPD coefficients is estimated from the stimulus $\boldsymbol{u}$ and the error $\boldsymbol{\epsilon} = \boldsymbol{z} - \boldsymbol{u}$. Minimizing $||\boldsymbol{\epsilon} - \boldsymbol{\Phi_u} \cdot \Delta\boldsymbol{\beta}||^2$ with the least-squares (LS) method, one has

$$\Delta\boldsymbol{\beta} = \left(\boldsymbol{\Phi_u}^H \boldsymbol{\Phi_u}\right)^{-1} \boldsymbol{\Phi_u}^H \boldsymbol{\epsilon}. \tag{2}$$

Then the DPD coefficients are updated with

$$\boldsymbol{\beta}_i = \boldsymbol{\beta}_{i-1} - \mu \cdot \Delta\boldsymbol{\beta}, \tag{3}$$

where $\mu < 1$ is the damping factor.

2) ILA: In the ILA case, a post-inverse block is estimated first. If the post-inverse block output is denoted by $\boldsymbol{z_p}$, $\boldsymbol{\beta}$ can be estimated by minimizing the error between $\boldsymbol{z_p}$ and $\boldsymbol{x}$. As $\boldsymbol{z_p} = \boldsymbol{\Phi_z}\boldsymbol{\beta}$ where $\boldsymbol{\Phi_z}$ is the matrix of basis functions for the normalized PA output signal $\boldsymbol{z}$, the LS estimate $\hat{\boldsymbol{\beta}}$ is obtained by substituting $\boldsymbol{\Phi_z}$ for $\boldsymbol{\Phi_u}$ and $\boldsymbol{x}$ for $\boldsymbol{\epsilon}$ in (2).

B. CFR

Traditional CFR approaches are HC and CAF. They usually operate on the signal $u(n)$ in front of the DPD. After a threshold is set, the CFR reduces the amplitude of signal peaks to the threshold.

1) HC algorithm: Hard clipping is the most basic CFR approach. If we clip the signal $u(n)$ with threshold P, the clipped signal can be represented as:

$$\mathrm{u_{HC}}(n) = \begin{cases} u(n)\frac{P}{|u(n)|}, & \text{if } |u(n)| \geq P \\ u(n), & \text{otherwise} \end{cases} \tag{4}$$

This generates unwanted distortion on adjacent channels, which degrades the linearization performance.

2) CAF algorithm: In order to remove out-of-band frequency components, a filter that has the same bandwidth as $\boldsymbol{u}$ is applied on the correction signal

$$c(n) = \mathrm{HC}(u(n)) = u(n) - \mathrm{u_{HC}}(n), \tag{5}$$

where $\mathrm{HC}(\cdot)$ represents the correction signal after hard-clipping. The signal clipped by the CAF approach is obtained by

$$\mathrm{u_{CAF}}(n) = u(n) - \mathrm{filter}\{c(n)\}. \tag{6}$$

However new peaks may be generated by filtering. Iterative clip-and-filter repeats the procedure for a certain number of iterations. If there are still new peaks generated at the last iteration, hard clipping is applied in the end. Since the number of peaks is reduced after each iteration, HC at the end is tolerable.

One can use CFR to reduce the PAPR of the PA input signal with two objectives in mind. Firstly, if the peak power is unchanged, the input average power increases so that the PA can work with higher efficiency. Secondly, the PA needs to be protected from the DPD-avalanche [10]: as the PA compresses the signal, the DPD expands it, which may cause divergence issues.

As a consequence, although the CFR is usually applied at the DPD input, there are actually two approaches to apply the CFR as shown in Fig 3: in front of the DPD or behind the DPD. In the former case, CFR is applied on the stimulus $u(n)$, the DPD input signal is denoted by $u_c(n)$, and the CFR threshold is determined by $P_{\mathrm{DPDinPeak}}$. In the latter case, CFR is applied on the DPD output signal $x(n)$, and the PA input signal is denoted by $x_c(n)$. The CFR threshold is determined by P_{PAinPeak}.

C. MCFR: a joint CFR/DPD approach

Like the DPD, the CFR can be implemented as a parametric model. In [7], an MCFR is proposed where the CFR input is the stimulus $\boldsymbol{u}$ and its output is the correction signal for the DPD output as in Fig 4.

The CFR and DPD coefficients (denoted by α and β respectively) are estimated iteratively using a closed-loop direct learning architecture as introduced in Section II-A1. At the i-th iteration, the bias $\Delta\boldsymbol{\beta}$ of DPD coefficients is estimated as (2). The bias $\Delta\boldsymbol{\alpha}$ of CFR coefficients is estimated

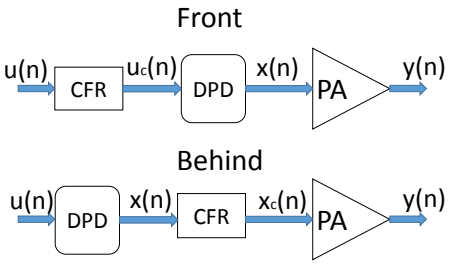

Fig. 3: CFR/DPD principle

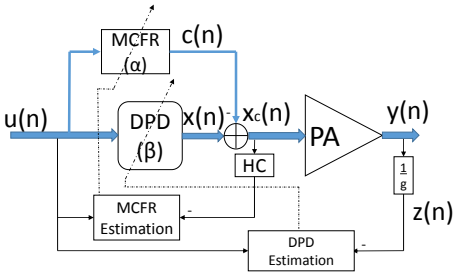

Fig. 4: "Behind DLA" CFR approach in [7]

according to the stimulus $u(n)$ and the clipped error signal $\epsilon_c(n) = \mathrm{HC}(x_c(n))$. Then the coefficients are updated as follows:

$$\begin{aligned} \boldsymbol{\alpha}_i &= \boldsymbol{\alpha}_{i-1} + \mu_1 \Delta\boldsymbol{\alpha} \\ \boldsymbol{\beta}_i &= \boldsymbol{\beta}_{i-1} - \mu_2(\Delta\boldsymbol{\beta} + \boldsymbol{\alpha}_{i-1}) \end{aligned} \tag{7}$$

where $\mu_{1,2} < 1$ are damping coefficients. As the output of the CFR block is the correction signal for the predistorted signal, we name this approach "Behind DLA".

Similarly to conventional approaches we may consider applying MCFR on the DPD input to get a "Front DLA" approach, as illustrated in Fig 5. The CFR block generates the correction signal $c(n)$ for the stimulus $u(n)$ and the estimation of $\Delta\boldsymbol{\alpha}$ is based on the stimulus $u(n)$ and the clipped error signal $\epsilon'_c(n) = \mathrm{HC}(u_c(n))$.

Both "Behind DLA" and "Front DLA" approaches suffer from the drawback of closed-loop DLA that the coefficient estimation needs iterations to converge. Moreover the structure of the CFR model should be the same as the DPD model according to (7).

III. MCFR WITH ILA

There have been very few studies on MCFR in the literature. In order to complete the study of different CFR approaches, we propose to identify the MCFR using ILA. Like the other approaches it can be implemented in front of or behind the DPD.

The correction signal generated by MCFR can be rewritten using matrix notation for the block of N samples:

$$\boldsymbol{c} = \boldsymbol{\Phi}_{\boldsymbol{u}}\boldsymbol{\alpha}. \tag{8}$$

The identification of ILA is introduced in Section II-A2. In the case where the MCFR is applied on the stimulus $u(n)$ ("Front ILA"), we estimate $\boldsymbol{\alpha}$ by minimizing the error between

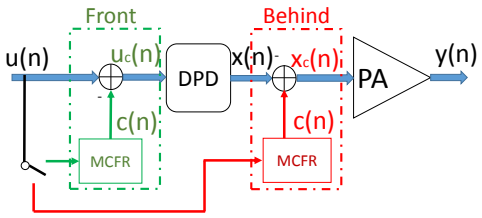

Fig. 5: "Front" and "Behind" MCFR structures

TABLE I: Number of FLOPs for operations

Operation	FLOPs	Operation	FLOPs
Real Addition	1	Real Multiplication	1
Real Division	4	Complex Addition	2
Complex Multiplication	6	Complex-Real Multiplication	2
Square-root	6~8		

$\boldsymbol{c}$ and $\boldsymbol{c_u}$ where $c_u(n) = \mathrm{HC}(u(n))$. The LS solution of (8) is here obtained by substituing $\boldsymbol{c_u}$ for $\boldsymbol{\epsilon}$ in (2).

In the case where the MCFR is applied on the DPD output $x(n)$ ("Behind ILA"), the CFR input is still $u(n)$. The CFR output now represents the correction signal for the DPD output $x(n)$. The LS solution $\hat{\alpha}$ is obtained in this case by substituting $\boldsymbol{c_x}$ for $\boldsymbol{\epsilon}$ in (2). The PA input is then the clipped predistorted signal

$$\boldsymbol{x_c} = \boldsymbol{x} - \boldsymbol{c}. \tag{9}$$

Contrary to DLA, as the CFR and DPD coefficients are identified separately, we can choose a different model structure for the CFR than that of the DPD.

IV. COMPLEXITY

The complexity of the different CFR approaches is evaluated in this section. As the identification of models can be off-line, here we consider only running complexity [11]. The DPD implementation is the same with the different CFR approaches. Thus its complexity is not taken into consideration.

The complexity of each approach is estimated by the number of FLOPs (floating-point operation) for the comparison. Table I shows the number of FLOPs for each operation that are used in the implementation [11]. As the square-root operation can be implemented with different algorithms, the number of FLOPs varies between 6 and 8. We considered an average of 7 FLOPs in the following calculations.

A. HC complexity estimation

In hard clipping, 1 complex modulus is needed to compare the amplitude of each sample with P.

If $u(n)$ can be decomposed as $u(n) = a(n) + i \cdot b(n)$, where $a(n)$ and $b(n)$ are the in-phase and quadrature components respectively, we have $|u(n)| = \sqrt{a(n)^2 + b(n)^2}$ which contains 2 real multiplications, 1 real addition and 1 square-root (10 FLOPs in total).

For those samples exceeding P, we need to implement also 1 real division (4 FLOP) and 1 complex-real multiplication (2 FLOPs), which makes 6 FLOPs in addition.

If the signal length is N and there are N_p peaks, we need $(10N + 6N_p)$ FLOPs. The number of clipped peaks depends on the threshold P.

B. CAF complexity estimation

With the CAF approach, the signal is clipped and filtered iteratively.

As with HC, one complex modulus of each sample is needed at each iteration. In our implementation, the peak windowing technique is taken in place of a low-pass filter to reduce the number of processed samples. We apply a Gaussian window on W samples centered at the clipped peak. Two complex subtractions (4 FLOPs) on each sample are implemented before and after filtering as (5) and (6). Denoting the average number of peaks per iteration as $\bar{N}_p$, the number of FLOPs at each iteration is $14N + \bar{N}_p(6 + 2W)$.

If we launch at most I_m iterations for CAF and there are still N'_p peaks at the end, the total number of FLOPs is

$$F_{\text{CAF}} = I_m[14N + \bar{N}_p(6 + 2W)] + (10N + 6N'_p). \quad (10)$$

C. MCFR complexity estimation

The complexity of the MCFR depends on its position.

In the case where the correction signal is applied at the DPD input, the complexity is that of a linear-in-parameter model, which corresponds to its number of coefficients. In [11], the running complexity of a model based on Volterra series is $N(8 \cdot N_c - 2)$, where the number of model coefficients is N_c and the signal length is N.

When the correction signal is applied at the DPD output, the clipped signal is expressed as (9). According to (1), (8) and (9), if the CFR and DPD models have the same structure, they can be merged:

$$\boldsymbol{x_c} = \boldsymbol{\Phi_u}(\boldsymbol{\beta} - \boldsymbol{\alpha}). \quad (11)$$

Thus MCFR is implemented along with DPD. The additional complexity brought by MCFR is only N_c complex additions which leads to $2N_c$ FLOPs.

V. Simulation Results

In this section, we test and compare the results of the different CFR approaches: HC, CAF, MCFR DLA, MCFR ILA, each of them is implemented in front of or behind the DPD.

We use a Wiener model PA for the simulation. A 20 MHz LTE signal is used as stimulus. Its peak-to-average power ratio (PAPR) at the 10^{-4} probability level is 8 dB. The signal length is 614400 samples. But we use only 25000 samples for DLA/ILA identifications.

As the DLA approach requires the DPD to have the same structure as CFR, we determine a GMP model structure using the algorithm in [12] for both CFR and DPD with DLA and ILA.

We aim at a gain g of the linearized PA equal to its small signal gain [9], which is 21 dB. The PA saturated output power is 24.79 dBm. Considering the PAPR of stimulus is 8 dB, we need to apply an OBO to avoid the PA saturation when

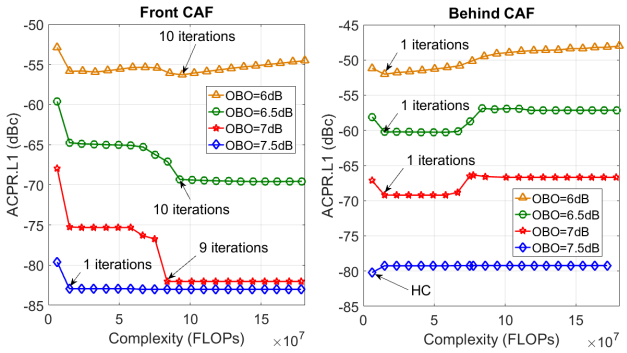

Fig. 6: ACPR vs CAF complexity

TABLE II: Impacts on PA linearity with different CFR approaches

OBO (dB)	ACPR.L1 (dBc): Front				ACPR.L1 (dBc): Behind			
	HC	CAF	ILA	DLA	HC	CAF	ILA	DLA
7.5	-78.9	-82.9	-76.7	-82.3	-80.2	-79.3	-76.1	-75.6
7	-67.9	-82.1	-70.5	-69.3	-67.1	-69.2	-67.8	-62.4
6.5	-59.6	-69.3	-61.1	-59.8	-58.0	-60.2	-58.4	-55.6
6	-52.9	-56.3	-55.1	-51.6	-51.2	-52.0	-54.3	-49.9

CFR is not applied. Thus the average DPD input power is set at -4.21 dBm if no CFR is applied. Applying CFR allows to reduce OBO to improve PA efficiency. Without a precise model for PA efficiency, we can consider it approximately linear to OBO (see [1] for instance, for an OFDM signal and a Doherty PA). Thus we represent the PA efficiency with OBO_{dB} in this paper.

In this section, the PA linearity is evaluated with the first lower adjacent channel power ratio (ACPR.L1) of the PA output signal spectrum. The ACPR.L1 at the output PA is -35.1 dBc and is decreased to -85.1 dBc after linearization with DPD only.

As the complexity of CAF is strongly influenced by its number of iterations I_m, we first make a test of its performance by varying I_m from 0 to 20. The case of 0 iteration is HC. The curves of ACPR versus CAF complexity are illustrated in Fig 6. The chosen I_m is taken considering the best ACPR performance and the lowest necessary complexity for all cases of OBO values. Therefore we launch 10 iterations for "Front CAF" and 1 iteration for "Behind CAF". The width of the Gaussian window is set at $W = 100$.

The results are given and discussed in the following.

Table II gives the details of the ACPR for all OBO values tested. When OBO increases, the differences between ACPR of different CFR approaches become larger. Only ACPR values are considered since all methods present low EVM values ($< 3\%$). "Front CAF" has the best linearization performance especially when OBO is larger than 6.5 dB. For MCFR ILA, the linearity does not change much with the position. On the other hand, "Front DLA" is close to "Front ILA" but "Behind DLA" is a little worse than "Behind ILA".

All approaches except HC have better linearization performances for "Front" position than "Behind". This is because, in the "Behind" case, the PAPR of the predistorted signal is largely extended by DPD. Though the threshold of "Behind" CFR is higher, the reduction of PAPR needed is greater than

TABLE III: Number of FLOPs of CAF

CFR approaches	HC	CAF		MCFR	
		Front	Behind	Front	Behind
F (FLOPs)	$6.1e^6$	$9.2e^7$ ~$1.5e^8$	$1.5e^7$	$1.46e^8$	60

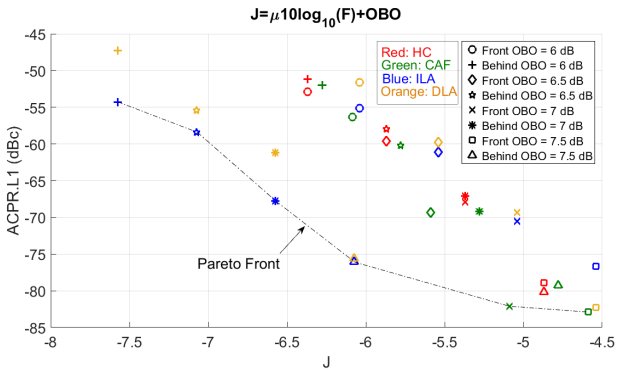

Fig. 7: ACPR at PA output after different CFR/DPD approaches versus merit values

in the "Front" case.

The complexity F of these approaches is computed with $N = 614400$. The number of peaks N_p for HC is counted in the simulation. For CAF, $\bar{N}_p$ and $\bar{N}'_p$ are also based on simulation. The results are given in Table III.

The complexity of HC is not much influenced by OBO values because the number of operations on clipping peaks is very limited. That is not the case for CAF as the filtering brings an important number of operations. The less the OBO is, the more peaks are detected, and thus the more complexity is demanded.

The model used for MCFR and DPD has $N_c = 30$ coefficients in this implementation. Since we only consider running complexity, the complexities of MCFR is the same with DLA or ILA. "Behind MCFR" is in parallel with the DPD and can be integrated in the DPD implementation by summing their coefficients. Note that the complexity of HC is very low compared with that of the DPD ($1.46e^8$ FLOPs).

To characterize the benefit of the CFR in terms of its ability to improve PA efficiency for a given complexity F, we propose a merit function to minimize:

$$J = 10\log_{10}(F^{\mu} \cdot \mathrm{OBO}_{\mathrm{lin}}) = \mu 10\log_{10}(F) + \mathrm{OBO}_{\mathrm{dB}}, \tag{12}$$

where μ is a weighting coefficient given by the ratio between the maximum variations of $\mathrm{OBO}_{\mathrm{dB}}$ and $10\log_{10}(F)$.

PA linearity versus merit for different OBO values is illustrated in Fig 7 ($\mu = 0.024$). In this two-objective optimization problem, we can find the Pareto front where the points are better than others either in ACPR or in merit value. The Pareto front consists of 6 points. Among them, 4 blue points result from the proposed "Behind ILA" approach and are characterized by a good merit, 2 green points result from "Front CAF" and are characterized by a good linearity. With a strong ACPR limitation, "Front CAF" with high OBO is needed. If more importance is given to CFR complexity and PA efficiency, "Behind ILA" MCFR is the best solution.

VI. Conclusion

In this paper we compared different CFR approaches by studying their impact on linearity for several OBO values, in the presence of DPD. The added computational burden is also taken into account. It leads to an increase in power consumption of the digital part that could potentially negate the improvement of the PA power efficiency. Traditional HC and CAF are included as well as a joint CFR-DPD method which we dubbed as MCFR. A novel MCFR technique with ILA is also proposed. Applying the correction signal generated by a MCFR on the predistorted signal can greatly reduce the complexity by trading off some linearity. Based on an estimation of the CFR computational complexity, we introduced a figure of merit to study the trade-off between linearity and overall power efficiency. The effectiveness of the proposed method in terms of trade-off among linearity, PA power efficiency and CFR complexity is confirmed. Future works include improving the ACPR by proposing appropriate models as well as a more precise estimation of the overall power efficiency through designing the implementations of the CFR and the DPD.

References

[1] S. Boumard, M. Lasanen, O. Apilo, A. Hekkala, C. Cassan, J. P. Verdeil, J. David, and L. Pichon, "Power consumption trade-off between power amplifier obo, dpd, and clipping and filtering," in *2014 26th International Teletraffic Congress (ITC)*, Sept 2014, pp. 1–5.

[2] J. Chani-Cahuana, M. Ozen, C. Fager, and T. Eriksson, "Digital predistortion parameter identification for rf power amplifiers using real-valued output data," *IEEE Trans. Circuits Syst. II, Exp. Briefs*, vol. 64, no. 10, pp. 1227–1231, Oct 2017.

[3] P. Suryasarman, P. Liu, and A. Springer, "Optimizing the identification of digital predistorters for improved power amplifier linearization performance," *IEEE Trans. Circuits Syst. II, Exp. Briefs*, vol. 61, no. 9, pp. 671–675, Sept 2014.

[4] A. Barakat, M. Thian, and V. Fusco, "A high-efficiency gan doherty power amplifier with blended class-ef mode and load-pull technique," *IEEE Trans. Circuits Syst. II, Exp. Briefs*, vol. 65, no. 2, pp. 151–155, Feb 2018.

[5] J. Wood, *Behavioral Modeling and Linearization of RF Power Amplifiers:*, ser. Artech House Microwave Library. Artech House, 2014.

[6] F. Sandoval, G. Poitau, and F. Gagnon, "Hybrid peak-to-average power ratio reduction techniques: Review and performance comparison," *IEEE Access*, vol. 5, pp. 27 145–27 161, 2017.

[7] R. N. Braithwaite, "A combined approach to digital predistortion and crest factor reduction for the linearization of an rf power amplifier," *IEEE Trans. Microw. Theory Techn.*, vol. 61, no. 1, pp. 291–302, Jan 2013.

[8] M. Abi Hussein, V. Bohara, and O. Venard, "On the system level convergence of ila and dla for digital predistortion," in *Wireless Communication Systems (ISWCS), 2012 International Symposium on*, Aug 2012, pp. 870–874.

[9] S. Wang, M. A. Hussein, O. Venard, and G. Baudoin, "Impact of the normalization gain of digital predistortion on linearization performance and power added efficiency of the linearized power amplifier," in *2017 12th European Microwave Integrated Circuits Conference (EuMIC)*, Oct 2017, pp. 310–313.

[10] A. Mbaye, G. Baudoin, A. Gouba, Y. Louet, and M. Villegas, "Combining crest factor reduction and digital predistortion with automatic determination of the necessary crest factor reduction gain," in *2014 44th European Microwave Conference*, Oct 2014, pp. 837–840.

[11] A. S. Tehrani, H. Cao, S. Afsardoost, T. Eriksson, M. Isaksson, and C. Fager, "A comparative analysis of the complexity/accuracy tradeoff in power amplifier behavioral models," *IEEE Trans. Microw. Theory Techn.*, vol. 58, no. 6, pp. 1510–1520, June 2010.

[12] S. Wang, M. A. Hussein, O. Venard, and G. Baudoin, "A novel algorithm for determining the structure of digital predistortion models," *IEEE Trans. Veh. Technol.*, pp. 1–1, 2018.